

Title

Leakage of old carbon dioxide from a major river system in the Canadian Arctic

Authors

Sanjeev Dasari^{1*}, Mark H. Garnett², Robert G. Hilton^{1*}

Affiliations

¹Department of Earth Sciences, University of Oxford, Oxford, OX1 3AN, UK

²NEIF Radiocarbon Laboratory, SUERC, Rankine Avenue, East Kilbride, G75 0QF

**To whom correspondence should be addressed:*

sanjeev.dasari@earth.ox.ac.uk; robert.hilton@earth.ox.ac.uk

Author Contributions

RG.H. designed the research; RG.H. conducted fieldwork; MH.G. and RG.H. conducted the laboratory analysis; S.D. and RG.H. analyzed the data; S.D. drafted the paper with input from all co-authors.

Competing Interest Statement

The authors declare no competing interest.

Data Availability Statement

All data is included in the manuscript and/or supporting information.

Classification

Major category: Physical Sciences

Minor category: Earth, Atmospheric, and Planetary Sciences

Keywords

Dissolved Inorganic Carbon, Carbon Isotopes, Permafrost, Arctic Carbon Cycle, CO₂ evasion

This PDF file includes

Main Text

Figures 1 to 5

1 Abstract

2 The Canadian Arctic is warming at an unprecedented rate. Warming-induced permafrost thaw can
3 lead to mobilization of aged carbon from stores in soils and rocks. Tracking the carbon pools supplied
4 to surrounding river networks provides insight on pathways and processes of greenhouse gas release.
5 Here, we investigated the dual-carbon isotopic characteristics of the dissolved inorganic carbon (DIC)
6 pool in the main stem and tributaries of the Mackenzie River system. The radiocarbon (^{14}C) activity
7 of DIC shows export of 'old' carbon (2380 ± 1040 ^{14}C years BP on average) occurred during summer
8 in sampling years. The stable isotope composition of river DIC implicates degassing of aged carbon
9 as CO_2 from riverine tributaries during transport to the delta, however, information on potential
10 drivers and fluxes are still lacking. Accounting for stable isotope fractionation during CO_2 loss, we
11 show that a large proportion of this aged carbon (60 ± 10 %) may have been sourced from biospheric
12 organic carbon oxidation, with other inputs from carbonate weathering pathways and atmospheric
13 exchange. The findings highlight hydrologically connected waters as viable pathways for
14 mobilization of aged carbon pools from Arctic permafrost soils.

16 Significance Statement

17 Warming of the circumpolar north can lead to the release of carbon stocks from thawing of organic-
18 rich permafrost soils and enhanced chemical weathering of rocks. Here, by tracing the isotopic
19 fingerprints of dissolved inorganic carbon pool in a northern Canadian Arctic River system, we show
20 that transfer of old C occurred on two separate occasions. The evading CO_2 in the river system is
21 plausibly sourced from the oxidation of aged organic matter, representing a leak of carbon from
22 millennial terrestrial C stocks through hydrologically connected waters. Such C mobilizing pathways
23 are of concern for future climate warming of permafrost zones. There is therefore an urgent need to
24 better understand the drivers of greenhouse gas release in such climatically vulnerable regions.

1 Main Text

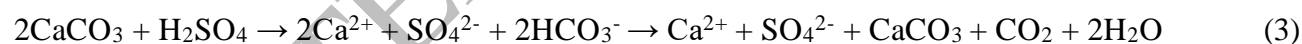
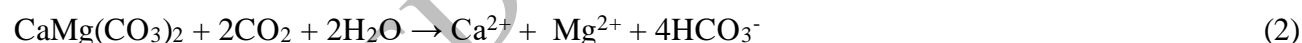
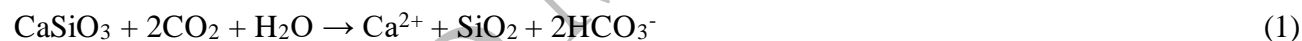
2 Introduction

3 Accelerated rates of climate warming in the high latitudes are likely to induce acute changes
4 in the major components of the Arctic cryosphere^{1,2}. In northern Canada, the annual average air
5 temperature has increased 2.3°C over the period of 1948–2016 and is projected to increase 7.8 °C by
6 2081–2100 relative to the period 1986–2005³. This could impact land-to-ocean transfer of
7 biogeochemical components, with implications for the environment, ecosystem, and broad-scale
8 Arctic biogeochemical cycling. One such component, the Arctic carbon cycle, is prone to various
9 processes influenced by warming⁴. In the circumpolar north, peat deposits and deltaic sediments have
10 accumulated organic-rich permafrost soils over millennia^{5–7}. Warming-induced permafrost thaw and
11 subsequently increased soil respiration could eventually lead to the release of greenhouse gases (e.g.,
12 CO₂, CH₄) through microbial decomposition and/or photodegradation, thereby exacerbating future
13 climate change^{8,9}. Changes in hydrology and the nature of mineral-water interactions following
14 permafrost thaw, alongside warming-induced changes to plant distribution and physiology, could also
15 contribute to enhanced chemical weathering and rock carbon inputs, which transfer carbon on
16 timescales of 10⁴–10⁶ years^{10,11}. Both these processes (i.e., old soil respiration and chemical
17 weathering) could potentially be active in certain northern landscapes^{e.g.,12}. Tracking the age and fate
18 of the carbon pool in river systems remains a priority for future projections of Arctic warming and
19 climate change. Currently, process-level understanding remains elusive and is hampered by the
20 challenges of sample collection from remote locations^{13–15}.

21 Rivers, dubbed as ‘biogeochemical reactors’, integrate the
22 characteristics of the surrounding landscapes, and are not exempt from the impacts of global warming
23 and climate change¹⁶. As such, it is possible to track vital information about C-dynamics from the
24 basin-specific characteristics of the organic and inorganic carbon pools, including particulate (POC)
25 and dissolved organic carbon (DOC) and dissolved inorganic carbon (DIC)^{e.g.,12,17–19}. In particular, the
26 application of radiocarbon has shed new light on the age, source and pathways of carbon in these
27 pools^{e.g.,18,19}. Here, we focus on the Mackenzie River basin and its associated tributaries (total
28 drainage area 1.8 × 10⁶ km²) as the largest contributor of freshwater and DIC and second largest
29 contributor of DOC, and as such a major carbon source from the North American continent to the
30 Arctic Ocean^{12,18}. The Mackenzie River basin exhibits varied soil organic matter content and is
31 dominated by sedimentary rock lithologies, with half of the basin lying within permafrost covered
32 zones (Figure 1). Two of its large tributaries (Arctic Red: 21.8 × 10³ km²; Peel River: 70.6 × 10³ km²)
33 almost exclusively drain continuous permafrost¹². Several works exist on the sources and fluxes of

1 DOC in Arctic rivers, justified by its link to changing hydrological pathways and its potential
2 reactivity^{e.g.,19-21}. In the Mackenzie River, analysis of long-term records in the main stem has
3 established increasing DOC (and DIC) fluxes in the past decades¹², while radiocarbon (¹⁴C) activity
4 of DOC suggests a mostly ‘modern’ origin, implying that vegetation and soil derived, rapidly cycling,
5 young organic matter likely dominates DOC in this river basin^{18,21}. This contrasts starkly with the
6 POC pool, which has a ¹⁴C composition reflecting erosion of aged soil organic matter and rock
7 organic carbon inputs^{18,19,21}. In stark contrast, there are no measurements of the age of one of the
8 major carbon pools, DIC, in this river basin, reflecting a broader deficit of radiocarbon DIC
9 measurements in the northern latitudes (> 60 °N)^{22,23}. We aim to address this major knowledge gap to
10 better understand the riverine C-export in one of the world’s most climatically vulnerable regions.

11 The DIC pool is influenced by a mixture of sources and processes. Chemical weathering of
12 carbonate and silicate minerals by carbonic acid contribute importantly to the DIC pool^{11,24,25}, with
13 DIC mostly in the form of bicarbonate (HCO₃⁻) whose production represents a CO₂ sink (Eq [1-2]). In
14 the Mackenzie River basin and other locations where sedimentary rocks dominate the lithology
15 (Figure 1), sulfide mineral (e.g., pyrite) oxidation is a pathway for carbonate dissolution, potentially
16 contributing to the present day HCO₃⁻ flux, (Eq [3])^{12,24-26}, or this CO₂ may be released to the
17 atmosphere at the reaction site²⁷



21 However, this weathering-derived bicarbonate is not conservative, and there could be large
22 influxes of CO₂ into the DIC pool from temperature-dependent decomposition of soil organic
23 matter^{26,28} or within river heterotrophic respiration¹⁶. In some less turbid rivers, uptake of CO₂ by
24 aquatic photosynthesis may also be important²⁹. In terms of inputs from the catchment, the CO₂
25 produced in near-surface soil includes autotrophic respiration of rapidly cycling carbon as well as
26 heterotrophic decomposition of carbon that cycles on a broad range of timescales²⁸. In the lower
27 depths of the seasonally thawed active layer, however, carbon that has cycled on millennial
28 timescales may decompose under aerobic and thawed conditions and seep into the interconnected
29 hydrological network^{13,14,19}. As such, it is expected that both ‘modern’ and ‘aged’ CO₂ are
30 exchanging C within the Mackenzie River DIC pool, respectively (Figure 2). Most river systems have
31 been found to be supersaturated in dissolved CO₂ relative to the atmosphere, meaning they act as a
32 large global source³⁰. With such diverse sources of riverine DIC (and CO₂) in this river system, it is
33 challenging to resolve the potential drivers using only source markers or conservative tracers.

1 Dual-carbon isotopic probing using stable carbon isotope ($\delta^{13}\text{C}$) and
2 radiocarbon ($\Delta^{14}\text{C}$) may contain information attributable to DIC source identification^{e.g.,26,31}. In the
3 past, such measurements have also provided valuable information on the residence times,
4 transformations, and interactions of other carbon reservoirs³²⁻³⁴. Therefore, we collected DIC samples
5 for $\delta^{13}\text{C}$ and $\Delta^{14}\text{C}$ from the Mackenzie River mainstem and its northern tributaries, the Peel and
6 Arctic Red rivers (Figure 1). The samples in the present study can be placed in the context of the
7 large existing body of work on the river POC^{18,21} and DOC^{17,19} alongside constraints on chemical
8 weathering^{11,12,24,25}, allowing us to investigate the origin of DIC in this high-latitude Arctic river
9 network and the implications for CO_2 released from river surfaces.

11 Results

12 The DIC concentrations, $\delta^{13}\text{C}_{\text{DIC}}$ and $\Delta^{14}\text{C}_{\text{DIC}}$ values ranged between 12 to 21 mg/L, -6.4 ‰ to
13 -2.1 ‰ and -179 ‰ to -134 ‰ in the Mackenzie River samples from upstream of the delta
14 (Tsiigehtchic) and in the Middle Channel of the delta, respectively. In comparison, the Arctic Red
15 River, Peel River and Peel River tributaries, the DIC concentrations, $\delta^{13}\text{C}_{\text{DIC}}$ and $\Delta^{14}\text{C}_{\text{DIC}}$ values
16 ranged between 9 to 33 mg/L, -10.2 ‰ to -0.2 ‰ and -434 ‰ to -130 ‰, respectively (Figure 3;
17 Tables S1-S2). On average, the observed $\Delta^{14}\text{C}_{\text{DIC}}$ in the Mackenzie River system (-250 ± 93 ‰, with
18 standard deviation range, $n = 17$ Figure 3) was found to be much lower than the reported $\Delta^{14}\text{C}_{\text{DIC}}$ in
19 e.g., streams (-112 ± 113 ‰)³¹, tropical rivers (43 ± 73 ‰)²⁶ and sea and ocean surfaces (-79 ± 108
20 ‰)³⁴. Here, a characteristic difference is the presence of aged DIC, with the radiocarbon ages ranging
21 between 1060 and 4492 ^{14}C years BP (before present). To the best of our knowledge, such DIC ages
22 haven't been reported for any large northern river system to date³².

23 The observed $\delta^{13}\text{C}_{\text{DIC}}$ in the Mackenzie River system (-5 ± 3 ‰) was enriched yet comparable
24 to the reported $\delta^{13}\text{C}_{\text{DIC}}$ in e.g., tropical rivers (-11 ± 2 ‰)²⁶ and streams (-8 ± 1 ‰)³¹. The $\delta^{13}\text{C}_{\text{DIC}}$
25 values appear to overlap with the isotope end members for chemical weathering processes (Table S1-
26 S3). Decomposition of organic matter within river systems will also contribute to riverine DIC, and
27 hence alter DIC isotopic ratios. In such a scenario, the $\delta^{13}\text{C}_{\text{DIC}}$ from within-system organic matter
28 remineralization will be similar to the $\delta^{13}\text{C}$ signature of the riverine organic matter which reflects a
29 mixture of C_3 biomass dominated inputs (-25 ± 3 ‰; see POC and DOC in Table S3)^{18,19,26,35}. In
30 comparison, the observed $\delta^{13}\text{C}_{\text{DIC}}$ values in the Mackenzie River system are nearly ~ 20 ‰ enriched
31 overall. This could result from the predominance of a single DIC source with distinct $\delta^{13}\text{C}$ signature
32 e.g., carbonate weathering by sulfuric acid. Such a possibility exists given the pronounced multi-

1 decadal increase in sulfate flux of ~ 64% in this system¹². However, processes such as atmospheric
2 exchange (i.e., with soils and water) also fractionate $\delta^{13}\text{C}$ and could result in shifts in $\delta^{13}\text{C}_{\text{DIC}}$ during
3 riverine transport³⁶⁻⁴⁰, which we discuss in the next section.

4 The major ion concentrations ($[\text{Ca}^{2+}]$, $[\text{Mg}^{2+}]$, and $[\text{SO}_4^{2-}]$; Table S1) were comparable with
5 previously reported values in this river system¹². The observed values were highest in the Peel River
6 samples and lowest in the Mackenzie mainstem, which supports previous work highlighting high
7 rates of carbonate and sulfide mineral weathering in the Peel River^{12,24,25} (Figure 1b). The ratios of
8 these ions and DIC are used to track the relative importance of chemical weathering. In particular, we
9 note a significant positive correlation between weathering components (Ca^{2+} , Mg^{2+} , SO_4^{2-}) and
10 $\Delta^{14}\text{C}_{\text{DIC}}$ ($R^2 > 0.9$, $p < 0.001$; Figure 4, see also Figure S1).

11 Discussion

12 The averaged $\Delta^{14}\text{C}_{\text{DIC}}$ values in global large rivers has been found to be $-32 \pm 140 \text{‰}$ ³². The
13 aged DIC we have observed in the Mackenzie River system ($\Delta^{14}\text{C}_{\text{DIC}} = -250 \pm 93 \text{‰}$, or 2380 ± 1040
14 ^{14}C years BP on average) has not been documented previously in any large Arctic rivers^{17,32}. To
15 explain the aged DIC, here we consider the DIC and CO_2 inputs and losses which may occur
16 throughout this northern landscape (Figure 2). First, we calculate a ‘predicted’ DIC isotopic
17 composition expected for the known chemical weathering pathways of rocks in the landscape. From
18 this starting point, we then explore how CO_2 inputs from organic matter respiration and
19 decomposition, either sourced in the landscape and/or within the river water, may contribute to the
20 isotopic composition of the river DIC pool. The loss of CO_2 from river surfaces (CO_2 evasion) is also
21 considered, as it can induce stable isotope fractionation, and the role of atmospheric CO_2 exchange
22 assessed. By considering these factors together, we put forward a hypothesis to explain the
23 Mackenzie River $\Delta^{14}\text{C}_{\text{DIC}}$ and $\delta^{13}\text{C}_{\text{DIC}}$ compositions, with old carbon source from a combination of
24 carbonate weathering inputs and aged carbon from organic matter degradation.

25
26
27 **Predicted DIC isotopic signatures from chemical weathering processes.** Previous work on the
28 Mackenzie River basin has quantified the fluxes of CO_2 drawdown and bicarbonate production by
29 carbonate and silicate weathering^{11,24,25}. Weathering of sedimentary rocks dominates the dissolved
30 cation load in this river system²⁵. Based on mass balance of dissolved weathering products from
31 previous work^{11,24,25}, an estimated 48% of the DIC pool should have been derived from carbonate
32 mineral weathering with carbonic acid, likely derived from atmospheric, soil CO_2 , and potentially
33 from rock organic carbon oxidation²⁵. An additional 38% of the DIC flux is attributed to carbonate

1 weathering by sulfuric acid²⁴. A further 14% of DIC is derived from silicate mineral weathering by
2 carbonic acid. Rock organic carbon oxidation has been quantified in this basin, but the fate of the CO₂
3 remains uncertain¹⁸. It could enter the DIC pool, or be released directly as atmospheric CO₂²⁷. If
4 entering the DIC pool, this would offset the atmospheric CO₂ used in carbonic acid weathering of
5 carbonate and silicate minerals (see Table S4). This would equate to 11% of the carbonic acid
6 weathering pool deriving from rock organic carbon oxidation, with the remaining 51% assumed to
7 derive from atmospheric or soil CO₂. Coupling these contributions to their respective dual-isotopic
8 signatures leads to a predicted DIC isotopic signature ('DIC_{predicted}' in Figure 3; Table S4).

9 The DIC_{predicted} value cannot explain the measured DIC isotopic compositions. The river DIC
10 is much younger than that expected for weathering inputs (Figure 3). However, a clear imprint of
11 weathering can still be seen on the $\Delta^{14}\text{C}_{\text{DIC}}$ by examining the dissolved ion loads. Correlations
12 between carbonate and sulfide mineral weathering products and the DIC radiocarbon activity are
13 found (Figure 4). The most ¹⁴C-depleted samples generally have the highest (Ca²⁺ + Mg²⁺)/DIC and
14 (Ca²⁺ + SO₄²⁻)/DIC values, and these come from the tributaries of the Peel River where carbonate and
15 sulfide weathering are widespread²⁴. These general patterns (between $\Delta^{14}\text{C}_{\text{DIC}}$ and carbonate
16 dissolution) have also been reported from the Amazon River³³ and Tibetan Plateau streams⁴⁰. While
17 this suggests an important weathering input to the modern DIC pool of the Mackenzie River system,
18 the DIC ages are not old enough to solely reflect the weathering inputs (e.g., the DIC_{predicted} ~ 6000
19 ¹⁴C years BP) and there is a large amount of variability in ¹⁴C age of DIC for a given dissolved
20 geochemical composition (Figure S1).

21 To explain the younger river DIC signal than predicted for chemical weathering inputs, we
22 have identified three possibilities. First, some of the CO₂ from carbonate weathering by sulfuric acid
23 and rock organic matter oxidation may not enter the DIC pool, as suggested by outcrop scale
24 measurements of shale weathering^{27,41}. This would act to increase the (Ca²⁺ + Mg²⁺)/DIC but we
25 would not find the carbonate weathering $\Delta^{14}\text{C}$ signature in the DIC pool. Second, we could invoke
26 atmosphere exchange. Isotope exchange between river DIC and atmospheric CO₂ would act to
27 increase $\Delta^{14}\text{C}_{\text{DIC}}$, but would not influence (Ca²⁺ + Mg²⁺)/DIC ratios. While both processes could be
28 acting, they cannot explain the other main feature of the dataset: the negative linear relationships
29 between river $\Delta^{14}\text{C}_{\text{DIC}}$ and (Ca²⁺ + Mg²⁺)/DIC and (Ca²⁺ + SO₄²⁻)/DIC (Figure 4). These relationships
30 suggest that as DIC increases relative to Ca²⁺ and Mg²⁺, $\Delta^{14}\text{C}_{\text{DIC}}$ increases. In other words, DIC
31 enrichment from a carbon source with a 'younger' $\Delta^{14}\text{C}_{\text{DIC}}$ value could explain the linear trends.
32 Based on regressions to the data, this DIC input appears to have a $\Delta^{14}\text{C}$ value < 0 ‰ (see x intercept
33 in Figure 4). Therefore, the third option to explain the geochemical data is that there is an important
34 input of DIC from plausibly biospheric organic carbon (see Figure 3).

1
2 **DIC input from the biospheric organic carbon oxidation.** The presence of aged DIC in this high-
3 latitude river system is likely given the large volumes of organic matter in soils, and the pathways of
4 organic carbon transfer from soil to streams (Figure 2). The oxidation of biospheric organic matter in
5 the landscape could deliver CO₂ to the river DIC pool via hydrological pathways⁴²⁻⁴⁴. Alternatively,
6 within river processing of a river DOC pool, or degradation of eroded organic matter in particulate
7 form (river POC) could add CO₂ to the river DIC pool.

8 Previous work has explored the mobilisation and age of DOC in the Mackenzie River and
9 found the majority of river DOC is young, with a similar $\Delta^{14}\text{C}$ value to atmospheric CO₂ in the year
10 of sampling^{17,19} (Figure 3a). However, a one-time input of aged DOC into the Mackenzie River
11 system was found in June 2018¹⁹ followed a pronounced warm temperature anomaly in winter
12 2017/2018 and an anomalous warm summer period in 2017 which was followed by colder summer
13 seasons in 2018 and 2019. During the DIC sampling periods in July 2013 and June 2017, neither a
14 temperature anomaly nor any broad-scale changes in the water discharge were encountered (Figure
15 S2) and at these times the sampled DOC was $\Delta^{14}\text{C}_{\text{DOC}} > 0 \text{ ‰}$ ¹⁹. The remineralisation or
16 photooxidation of allochthonous DOC could provide the additional DIC input we propose. However,
17 the DIC enrichment appears to have a $\Delta^{14}\text{C}_{\text{DIC}}$ value less than 0 ‰ (Figure 4). Interestingly, the
18 contrast between DIC and DOC ¹⁴C age suggests significant quantities of DIC cannot be the product
19 of autotrophic DOC uptake in the river at these sampling periods (i.e., primary production)²⁶.

20 A plausible pathway for DIC inputs is the leakage of CO₂ from organic-rich permafrost zones
21 carried by modified hydrological pathways⁴²⁻⁴⁴ (Figure 2). Long-term observations of air temperature
22 records from Inuvik and Norman Wells show temperature increases over the last 76 years during the
23 freezing season (Figure S2). This influences the dynamics and thickness of the active layer modulated
24 by the seasonally varying temperatures. Indeed, in the northern Mackenzie River basin, a thickening
25 of the active layer by about 10% has been reported since 2000⁴⁵. The development of thin, perennial
26 taliks within and above permafrost is ensued during the summer months from the vertically and
27 laterally thawing permafrost table. This thaw is sustained further with mild winters⁴⁶⁻⁴⁸. Increased
28 hydrological connectivity can then enhance drainage of surface soils, and consequently the organic
29 soils can be undersaturated prior to freeze back in fall⁴⁹. During spring and in this regime, a larger
30 portion of meltwater can thus infiltrate soils, supplying sensible heat to the soil and leading to the
31 thawing of the upper permafrost table, further expanding the hydrologically connected
32 pathways^{14,42,49}. CO₂ from soil respiration and decomposition below the active layer can thus be
33 mobilized by this subsurface flow of water. An additional coupled process could be the formation of
34 thermokarst erosion features, which also allows deep, old soil organic matter to be exposed to O₂ rich

1 atmosphere and waters^{14,44}. These mechanisms would result in subsequent transfer of dissolved CO₂
2 to the river system where it can exchange with the river DIC pool^{26,35,43}.

3
4 **Constraining the biospheric organic carbon oxidation isotopic endmember.** To quantify how
5 biospheric organic carbon oxidation may contribute to the DIC pool in the Mackenzie River, we need
6 to establish its radiocarbon and stable isotope composition. The $\Delta^{14}\text{C}$ signatures of CO₂ from soil
7 respiration and decomposition could have a wide range due to the decomposition of organic carbon
8 pools of varying age²⁸. Studies on the ¹⁴C content of respired soil CO₂ indicate that most soil
9 respiration is from organic matter sources with a $\Delta^{14}\text{C} > 0\text{‰}$, as also observed recently in a similar
10 northern site^{26,28,35}. However, an assessment of the influence of chemical weathering on the
11 Mackenzie River DIC radiocarbon content shows that in a no weathering-C input scenario, the river
12 $\Delta^{14}\text{C}_{\text{DIC}}$ still appears to be $< 0 \text{‰}$ (see x-intercept in Figure 4), implying that CO₂ from recent
13 ecosystem respiration (Figure 3) may not be a viable source in this case.

14 Soil pore CO₂ can contribute to riverine DIC. The $\Delta^{14}\text{C}$ of CO₂
15 in soil pores in permafrost-rich environments has been found to be older than in ecosystem
16 respiration³⁵. In fact, an overlap between the observed average $\Delta^{14}\text{C}_{\text{DIC}}$ in the Mackenzie River
17 system and the $\Delta^{14}\text{C}\text{-CO}_2$ soil pore is evident (Figure 3). Indeed, an emerging feature of permafrost
18 carbon feedback is the one of ‘lateral permafrost carbon mobilization’ wherein soil pore water
19 happens to be a key variable in the generation and terrestrial emission/transport of greenhouse gases
20 from thawing permafrost^{14,42-44}.

21 Currently, however, there is very limited
22 information on attributes of soil pore water (for example, changes in soil pore water pH during lateral
23 transport as in Figure 2) in the Mackenzie River system and in the northern regions in general^{12,14,35,42-}
24 ^{44,50}. A study of soil pore water characteristics in a transect of permafrost wetland in Greenland
25 suggests a dominance of lateral advection transport process in the mobilization of CO₂, providing
26 evidence of acidification of the permafrost table linked to CO₂ bubble ebullition⁴³. However, the
27 proportion of the DIC formed from exchange with soil pore CO₂ and the impact on the chemical
28 equilibrium of the carbonate system for river systems remain unknown.

29 We can provide additional constraint on the possible composition of CO₂ from biospheric
30 organic carbon oxidation by using the river POC load. The river POC in the Mackenzie system is
31 dominated by biospheric carbon from a mixture of plant detritus and degraded and aged organic
32 matter from soil (70-90% of the POC), alongside rock organic carbon inputs^{14,18,19}. The biospheric
33 POC has been derived eroded from a large spatial area across the catchments. The $\Delta^{14}\text{C}$ and $\delta^{13}\text{C}$
values of river POC (Figure 3a) can therefore provide additional constraint on the composition of CO₂

1 from biosphere organic carbon oxidation (see Table S3). Further research is warranted to better
2 understand the chemical and isotopic characteristics of this organic matter source in the context of
3 permafrost thaw and DIC in the Mackenzie River system.

4 Here, for this preliminary isotopic investigation of DIC from a northern river, we give equal
5 weight to the dual-isotopic signatures of river POC¹⁸ and CO₂ measured in northern peatland soil
6 pores³⁵ to define a varied biosphere organic carbon oxidation isotopic endmember. We report the
7 endmember as mean ± SD (Figure 3b, Table S3) of the available data from published works^{18, 35}. A
8 two-component mixing (Chemical weathering + Biosphere organic carbon oxidation) could partly
9 explain the observed $\Delta^{14}\text{C}_{\text{DIC}}$ in the Mackenzie River system. However, the average $\Delta^{14}\text{C}_{\text{DIC}}$ in the
10 Mackenzie River system is less aged than this predicted two-component mixing (Figure 3b). A three-
11 component mixing including atmospheric CO₂ ($\Delta^{14}\text{C} = \sim 20 \text{ ‰}$) could then explain the observed
12 $\Delta^{14}\text{C}_{\text{DIC}}$ values in the Mackenzie River system. While such a mixing is feasible, the observed dual-C
13 isotopic composition of river DIC is mostly outside this predicted three-component mixing triangle
14 (Figure 5a). We hypothesize that this could potentially be linked to the stable carbon isotopic
15 fractionation of DIC due to the outgassing of CO₂ from the river surface^{37,40}.

16
17 **A role for CO₂ evasion from the Mackenzie River.** To explain the observed $\delta^{13}\text{C}_{\text{DIC}}$ values, we
18 hypothesize that outgassing of CO₂ is a key contributor. River CO₂ in equilibrium with HCO₃⁻ has
19 lower $\delta^{13}\text{C}_{\text{DIC}}$ values, meaning release of CO₂ from river surfaces could drive the DIC pool to higher
20 $\delta^{13}\text{C}_{\text{DIC}}$ values. There are also potential fractionation effects at the water surface³⁶. To explore the role
21 of CO₂ evasion on the stable isotope composition, we calculate the excess *PCO₂* (*ePCO₂*) in the river
22 water i.e., the ratio of *PCO₂* in the sample calculated from field-determined pH and temperature to
23 that of the atmosphere. Measurement of pH during the sampling campaign allowed for the estimation
24 of *PCO₂* of the water samples as conducted elsewhere³⁷.

25 In general, CO₂ diffuses out of waters when the *PCO₂* of the solution is greater than
26 that of the ambient atmosphere^{16,30,37}. In the present dataset, the *ePCO₂* ranged between 1 and 3
27 (Figure 5b) which is comparable with previously reported *ePCO₂* values from the Mackenzie River
28 system⁵¹. It has been found that the isotopic fractionation of DIC due to CO₂ loss becomes significant
29 for *ePCO₂* of ~ 2 and above^{52,53}. Indeed, we find that as *ePCO₂* decreases, the $\delta^{13}\text{C}_{\text{DIC}}$ values increase
30 (Figure 5b). This suggests that loss of CO₂ from river surfaces lowers *ePCO₂* and impacts $\delta^{13}\text{C}_{\text{DIC}}$,
31 altering any primary source signal. Similar patterns have been linked to the evasion of CO₂ in
32 headwater catchment streams³⁷⁻⁴⁰. Also, other studies at carbonate springs and in acidic headwater
33 catchments have documented similar shifts in $\delta^{13}\text{C}_{\text{DIC}}$ due to CO₂ outgassing⁵³⁻⁵⁵. However, the extent

1 of the relationship between $ePCO_2$ and isotopic fractionation of HCO_3^- due to CO_2 loss remains
2 unknown for this river system.

3 In open systems, the kinetic isotopic fractionation associated with this process ($\epsilon_{HCO_3^- - CO_2}$) is
4 estimated to be $\sim 14.7\%$ ³⁸, which is greater than the reported equilibrium value of $\epsilon_{HCO_3^- - CO_2} = 8\%$ ⁵⁶⁻
5 ⁵⁸. Assuming this to be the case, we recalculate a minimum $\delta^{13}C_{DIC}$ value prior to CO_2 evasion in the
6 Mackenzie River main stem of $\sim -19 \pm 3\%$ (see 'DIC_{prior}' in Figure 5). We can also assess the
7 fractionation using the empirical data here (Figure 5). If we use the highest reported $ePCO_2 \sim 4$ from
8 the Mackenzie River system⁵¹, the value for isotopic fractionation is estimated (based on the
9 relationship in Figure 5b) to be $\sim -17\%$. These two approaches thus return near similar estimates of
10 stable isotope fractionation due to CO_2 evasion in the river system. The ^{14}C values undergo correction
11 for isotope fractionation as part of the reporting of radiocarbon measurements⁵⁹ wherein $\Delta^{14}C$
12 is 'normalized' where the effect of fractionation is removed, as such changes should not occur in
13 $\Delta^{14}C$ during CO_2 evasion. The release of CO_2 could be linked to the formation of secondary carbonate
14 minerals in rivers. However, many rivers around the world are over saturated with respect to
15 carbonate precipitation⁶¹, yet lack clear direct evidence for secondary river carbonates. This remains
16 an open question for the Mackenzie River system, although we note that secondary carbonate
17 precipitation coupled to CO_2 evasion would lead to minimal net shift in the $\delta^{13}C_{DIC}$ value of the total
18 DIC pool.

19 The sources of DIC can be re-assessed by considering our calculated $\delta^{13}C_{DIC}$ value of DIC_{prior},
20 assuming it has the same $\Delta^{14}C$ as DIC_{observed}. This correction now places the DIC_{prior} within the source
21 mixing triangle previously described (Figure 5a). The DIC_{prior} has shifted closer to the biosphere
22 organic carbon oxidation endmember, which can further explain the presence of observed carbon ages
23 in the Mackenzie River system. In other words, the CO_2 inputs from respiration of organic matter mix
24 are partly aged and mix with the old C sourced from carbonate weathering inputs. We also find a
25 potential role for isotopic exchange with the atmosphere (Figure 5a). A quantitative source
26 apportionment of the DIC_{prior} using Bayesian statistical approach (see Methods) suggests that
27 biosphere organic carbon oxidation could contribute as much as $60 \pm 10\%$ to the DIC in this river
28 system as a whole (Figure 5c). Together, this implies that aged CO_2 from the landscape is leaking
29 from the Mackenzie River system. This is likely happening during DIC transit from the tributaries to
30 the deltaic region (as witnessed in the decreasing radiocarbon age of DIC between the riverine
31 tributaries and main channel). It therefore appears that large-scale mobilization of greenhouse gases
32 from aged carbon pools in permafrost soils is viable through hydrologically connected waters and
33 degradation of river organic matter pools.

1 **Wider implications.** The aged carbon measured in the DIC pool of the Mackenzie River system can
2 be explained, once accounting for stable isotope fractionation during CO₂ release from rivers, as a
3 mixture of carbonate weathering processes and biospheric organic carbon oxidation (Figure 5a). The
4 oxidation of aged organic matter represents a leak of carbon from millennial storage on land, and is a
5 pathway of concern for future climate warming in permafrost zones⁹. Streams and rivers may be a
6 route of this old carbon out from deep soils, into an open system where *PCO₂* promotes river CO₂
7 release (Figure 5b). If the DIC from carbonate weathering is derived from sulfide oxidation, the
8 carbon is a leak of geological carbon⁷ and appears to be of similar magnitude to organic carbon
9 oxidation in the river system (Figure 5b). Enhanced sulfide oxidation coupled carbonate weathering
10 and organic matter oxidation have both been linked to increase temperature^{27,28,50}.

11 To understand the role of river CO₂ release in the modified biogeochemical cycles of the
12 Arctic we require more focus on the age and isotope composition of DIC. Seasonal and time-series
13 ¹⁴C-DIC samples, in analogy to sampling efforts made for DOC and POC¹⁹ are needed to shed light
14 on how changing hydrological pathways are modifying carbon pathways to river systems¹²⁻¹⁴.
15 Alongside these samples it is necessary to better understand the CO₂ release fluxes from river
16 surfaces. Potential factors such as DIC delivery, *PCO₂* gradient, pH and turbulence in the river likely
17 drive river CO₂ evasion^{17,26,30,37}. Such information is currently limited for the Mackenzie River
18 system, wherein measurements have been sparse and mostly concentrated at few locations e.g.⁵¹ and
19 not along the transect of the river e.g.⁶⁰. The role of secondary carbonate precipitation^{61,62} and its
20 influence on the fluxes and isotopic composition of CO₂ also remains unknown. Further investigation
21 of concentrations, fluxes, and isotopic composition of greenhouse gases is therefore much warranted
22 from this high Arctic river system and others, in order to better understand the drivers of greenhouse
23 gas release in such climatically-vulnerable northern frontiers.

24 **Materials and Methods**

25 **Sampling.** River samples were collected in July 2013 and June 2017. The July 2013 samples
26 are from high/receding water stage (Figure S2), for the Mackenzie River at Tsiigehtchic, in the Delta
27 (middle channel), the Peel River, Arctic Red River, and the tributaries of the Peel River (Figure 1). In
28 June 2017, the main sites (Mackenzie River at Tsiigehtchic and delta, the Peel River, Arctic Red
29 River) were resampled at high river flow, shortly after ice breakup (Figure S2). In order to assess any
30 potential vertical variation, we used a modified horizontally mounted ~5.1 L Niskin bottle to recover
31 water from different depths¹⁸. For DIC measurements, we followed the protocol of Bryant et al., 2013
32 (Ref. 63). One-litre capacity foil bags (FlexFoil PLUS), composed of 4 layers (polypropylene,
33

1 polyethylene, aluminium foil, and polyethylene), were adapted to allow easy introduction of liquid
2 sample. River water was filtered directly into weighed foil bags through polyethersulfone filters
3 (PES; Ø 142 mm, 0.22 µm). Prior to sample collection, each foil bag was sample-rinsed by attaching
4 the Tygon® tubing to the Niskin sampler tap, removing the clip on the Tygon tubing and allowing
5 approximately 50 mL of water to enter the bag, and then allowing the bag to drain. The foil bag was
6 then filled to ~200-500 ml depending on expected DIC concentrations (half the bag capacity) and
7 then, held with the outlet pointing upwards, the bag was gently squeezed so that the Tygon tubing
8 remained water-filled before reapplying the clip, to ensure no air was trapped in the sample bag. The
9 filled bag was re-weighed, and refrigerated in the dark at 4°C during fieldwork, shipped to the UK
10 and the sample was frozen within ~ 1 week of collection. Aliquots for ion analysis were collected in
11 acid-washed high-density polyethylene (HDPE) bottles following methods outlined in Horan et al.,
12 2019 (Ref. 25). Further sampling details can be found in the supporting information Table S1.
13

14 **Measurements.** Water-soluble ion measurements were carried out at Durham University in
15 the UK using a Dionex Ion Chromatography system (DX-120, ThermoScientific) with an analytical
16 reproducibility of 5%. Parameters such as water temperature and pH were measured onsite using
17 handheld probes calibrated each field day (Hannah Instruments pHep). The storage and hydrolysis of
18 the water samples for DIC concentration and isotopic measurements was based upon the method
19 described elsewhere⁶³ and conducted at NEIF Radiocarbon Laboratory in East Kilbride, UK. Briefly,
20 the cryogenic isolation of CO₂ from the water sample is achieved by introducing orthophosphoric
21 acid into the water sample transferred into a hydrolysis vessel⁶³. This CO₂ is passed through 2 dry ice-
22 ethanol cryogenic traps, followed by 2 liquid nitrogen traps to cryogenically isolate the evolved CO₂.
23 Pressure readings of the evolved CO₂ provide the DIC concentration.

24 Stable carbon isotope measurements were carried out on an aliquot of the recovered CO₂
25 using a dual-inlet stable isotope mass spectrometer (Thermo Fisher DELTA V Plus), calibrated with
26 international standards and reported as δ¹³C ‰ relative to Vienna Pee Dee belemnite (VPDB). A
27 second aliquot of the recovered CO₂ was converted to graphite by Fe/Zn reduction and measured for
28 ¹⁴C content on an Accelerator Mass Spectrometer (AMS; National Electrostatics Corporation, USA)
29 at the SUERC AMS Laboratory. The ¹⁴C data are reported as Δ¹⁴C, i.e. as per mil deviation from the
30 AD 1950 decay-corrected NBS oxalic acid standard⁵⁹. Further methodological details can be found
31 elsewhere⁶⁴.
32

1 **Bayesian statistical source apportionment.** By combining the dual isotope signatures ($\Delta^{14}\text{C}$ and
 2 $\delta^{13}\text{C}$) and assuming mass balance, it is possible to explore the relative contributions from various
 3 sources using a forward modeling approach:

$$4 \quad \begin{pmatrix} \Delta^{14}\text{C}_{\text{sample}} \\ \delta^{13}\text{C}_{\text{sample}} \\ 1 \end{pmatrix} = \begin{pmatrix} \Delta^{14}\text{C}_{\text{bio. C. oxdn.}} & \Delta^{14}\text{C}_{\text{chem. weath.}} & \Delta^{14}\text{C}_{\text{atm. C}} \\ \delta^{13}\text{C}_{\text{bio. C. oxdn.}} & \delta^{13}\text{C}_{\text{chem. weath.}} & \delta^{13}\text{C}_{\text{atm. C}} \\ 1 & 1 & 1 \end{pmatrix} \begin{pmatrix} f_{\text{bio. C. oxdn.}} \\ f_{\text{chem. weath.}} \\ f_{\text{atm. C}} \end{pmatrix}$$

5 Where f denotes the fractional contribution from a given source, sample denotes the value of
 6 the analyzed field sample and the other isotope-values are source signatures ('bio. C. oxdn.', 'chem.
 7 weath.' and 'atm. C' corresponding to biosphere organic carbon oxidation, chemical weathering, and
 8 atmospheric input respectively). Two main complexities exist for solving this forward mixing model.
 9 The first regards the variability in the isotopic signatures of $\Delta^{14}\text{C}$ and $\delta^{13}\text{C}$ of various source classes
 10 i.e., endmember variability (e.g., SI Table S3). The uncertainties in endmembers dominate over the
 11 measurement uncertainties. It is recognized that in order to correctly estimate the relative source
 12 contributions and related uncertainties, the endmember variability as well as other sources of
 13 uncertainty needs to be included in the analysis. While the biospheric organic carbon end member
 14 could be highly variable¹⁸, we conclude this mixing analysis is still worthwhile, to establish the
 15 potential input of this component.

16 Markov Chain Monte Carlo (MCMC)-driven Bayesian approaches have been
 17 implemented to account for multiple sources of uncertainties/variabilities^{65,66}. The MCMC approach
 18 used here was developed in detail in Andersson et al., 2015 and builds on Andersson et al 2011;
 19 https://github.com/mskoldSU/Andersson_et_al_2015 (open-access R-code) and has been used in
 20 multiple atmospheric aerosol studies^{e.g.68-70} as well as for other systems such as the isotope-based
 21 source apportionment of PAHs in 34 soils and the isotope-based source apportionment of organic
 22 carbon in sediments^{71,72}. The statistical treatment of the endmember variability (in this approach) is
 23 the same regardless if one separates liquid fossil vs coal in black carbon aerosols or permafrost vs
 24 plankton in marine sediments. The resulting probability density functions output from the model give
 25 a 'least-biased' representation of the precision. As such, here we have estimated the relative
 26 contributions from three likely sources to riverine DIC in the Mackenzie River system based on this
 27 approach (Figure 5c). The second complexity relates to processes which alter the stable isotope
 28 composition of DIC. As discussed in the main text, we provide a first order correction for
 29 fractionation due to CO_2 evasion and explore the resulting stable isotope composition with the mixing

1 model. Future work that independently quantifies the CO₂ evasion flux and its isotope composition, in
2 addition to denser sampling in space and time, should remain a research priority.

3 **Acknowledgments**

4 The authors acknowledge field support from the Aurora Research Institute, Inuvik, with research
5 conducted and samples collected under licences 15288 and 16106. We thank the Gwich'in Tribal
6 Council for their advice on working in the Mackenzie Delta region. Additional field support and
7 discussions are acknowledged from Ed Tipper (CAN13 campaign) and Edwin Amos, Mathieu
8 Dellinger, Christina Larkin and Melissa Schwab (CAN17 campaign). SD and RGH were funded by a
9 European Research Council (ERC) Consolidator Grant (CoG 2020) "RIV-ESCAPE", project number
10 101002563, to RGH. Radiocarbon measurements were part-funded by the UK Natural Environment
11 Research Council (NERC), Radiocarbon Facility allocation number 1999.0416 to RGH.

13 **References**

- 15 1. IPCC: Summary for Policymakers, in: Global Warming of 1.5 °C. An IPCC Special Report on the
16 impacts of global warming of 1.5 °C above pre-industrial levels and related global greenhouse gas
17 emission pathways, in the context of strengthening the global response to the threat of climate
18 change, sustainable development, and efforts to eradicate poverty, edited by: MassonDelmotte, V.,
19 Zhai, P., Pörtner, H.-O., Roberts, D., Skea, J., Shukla, P. R., Pirani, A., Moufouma-Okia, W., Péan,
20 C., Pidcock, R., Connors, S., Matthews, J. B. R., Chen, Y., Zhou, X., Gomis, M. I., Lonnoy, E.,
21 Maycock, T., Tignor, M., and Waterfield, T., Cambridge University Press, Cambridge, UK and New
22 York, NY, USA, 3–24, 2018.
- 24 2. IPCC: Summary for Policymakers, in: Climate Change and Land: an IPCC special report on climate
25 change, desertification, land degradation, sustainable land management, food security, and
26 greenhouse gas fluxes in terrestrial ecosystems, edited by: Shukla, P. R., Skea, J., Calvo Buendia, E.,
27 Masson-Delmotte, V., Pörtner, H.-O., Roberts, D. C., Zhai, P., Slade, R., Connors, S., van Diemen,
28 R., Ferrat, M., Haughey, E., Luz, S., Neogi, S., Pathak, M., Petzold, J., Portugal Pereira, J., Vyas, P.,
29 Huntley, E., Kissick, K., Belkacemi, M., and Malley, J., 2019.

3. Zhang, X., Flato, G., Kirchmeier-Young, M., Vincent, L., Wan, H., Wang, X., et al. 2019. Changes in temperature and precipitation across Canada; Chapter 4. In E. Bush & D. S. Lemmen (Eds.) *Canada's Changing Climate Report* 112–193. Ottawa, Ontario: Government of Canada.
4. McGuire, A.D., Anderson, L.G., Christensen, T.R., Dallimore, S., Guo, L., Hayes, D.J., Heimann, M., Lorenson, T.D., Macdonald, R.W. and Roulet, N., 2009. Sensitivity of the carbon cycle in the Arctic to climate change. *Ecological Monographs*, 79, 523-555.
5. Hugelius, G., Strauss, J., Zubrzycki, S., Harden, J. W., Schuur, E. A. G., Ping, C. L., et al. 2014. Estimated stocks of circumpolar permafrost carbon with quantified uncertainty ranges and identified data gaps. *Biogeosciences*, 11, 6573–6593.
6. Zimov, S. A., Schuur, E. A. G., & Stuart Chapin, F. III 2006. Permafrost and the global carbon budget. *Science*, 312, 1612–1613.
7. Zolcos, S., Tank, S.E. and Kokelj, S.V., 2018. Mineral weathering and the permafrost carbon-climate feedback. *Geophysical Research Letters*, 45, 9623-9632.
8. Ward, C. P., & Cory, R. M. 2016. Complete and partial photo-oxidation of dissolved organic matter draining permafrost soils. *Environmental Science and Technology*, 50, 3545–3553.
9. Schuur, E. A. G., Bockheim, J., & Canadell, J. 2008. Vulnerability of permafrost carbon to climate change: Implications for the global carbon cycle. *Biogeosciences*, 58, 701–714.
10. Beaulieu E, Godderis Y, Donnadiou Y, et al., 2012 High sensitivity of the continental-weathering carbon dioxide sink to future climate change *Nat. Clim. Change*, 2, 346–9.
11. Gaillardet, J., Dupre', B., Louvat, P., and Alle`gre, C. J., 1999, Global silicate weathering and CO₂ consumption rates deduced from the chemistry of large rivers: *Chemical Geology*, 159, 3–30.
12. Tank, S. E., Striegl, R. G., McClelland, J. W., & Kokelj, S. V. 2016. Multi-decadal increases in dissolved organic carbon and alkalinity flux from the Mackenzie drainage basin to the Arctic Ocean. *Environmental Research Letters*, 11, 054015.

- 1 13. Vonk, J. E., Mann, P. J., Davydov, S., Davydova, A., Spencer, R. G. M., Schade, J., et al. 2013. High
2 biolability of ancient permafrost carbon upon thaw. *Geophysical Research Letters*, 40, 2689–2693.
- 3
- 4 14. Vonk, J. E., Tank, S. E., Bowden, W. B., Laurion, I., Vincent, W. F., Alekseychik, P., et al. 2015.
5 Reviews and syntheses: Effects of permafrostthaw on Arctic aquatic ecosystems. *Biogeosciences*, 12,
6 7129–7167.
- 7
- 8 15. Turetsky, M. R., Abbott, B. W., Jones, M. C., Walter Anthony, K., Olefeldt, D., Schuur, E. A. G., et
9 al. 2019. Permafrost collapse is accelerating carbon release. *Nature*, 569, 32–34.
- 10
- 11 16. Battin, T.J., Lauerwald, R., Bernhardt, E.S., Bertuzzo, E., Gener, L.G., Hall Jr, R.O., Hotchkiss,
12 E.R., Maavara, T., Pavelsky, T.M., Ran, L. and Raymond, P., 2023. River ecosystem metabolism and
13 carbon biogeochemistry in a changing world. *Nature*, 613, 449-459.
- 14
- 15 17. Raymond, P. A., McClelland, J. W., Holmes, R. M., Zhulidov, A. V., Mull, K., Peterson, B. J., et al.
16 2007. Flux and age of dissolved organic carbon exported to the Arctic Ocean: A carbon isotopic
17 study of the five largest arctic rivers. *Global Biogeochemical Cycles*, 21, GB4011.
- 18
- 19 18. Hilton, R. G., Galy, V., Gaillardet, J., Dellinger, M., Bryant, C., O'Regan, M., et al. 2015. Erosion of
20 organic carbon in the Arctic as a geological carbon dioxide sink. *Nature*, 524, 84–87.
- 21
- 22 19. Schwab, M.S., Hilton, R.G., Raymond, P.A., Haghypour, N., Amos, E., Tank, S.E., Holmes, R.M.,
23 Tipper, E.T. and Eglinton, T.I., 2020. An abrupt aging of dissolved organic carbon in large Arctic
24 rivers. *Geophysical Research Letters*, 47, GL088823.
- 25
- 26 20. Matsuoka, A., Babin, M. and Vonk, J.E., 2022. Decadal trends in the release of terrigenous organic
27 carbon to the Mackenzie delta (Canadian arctic) using satellite ocean color data (1998–
28 2019). *Remote Sensing of Environment*, 283, 113322.
- 29
- 30 21. Campeau, A., Soerensen, A.L., Martma, T., Åkerblom, S. and Zdanowicz, C., 2020. Controls on the
31 ¹⁴C content of dissolved and particulate organic carbon mobilized across the Mackenzie River
32 Basin, Canada. *Global Biogeochemical Cycles*, 34, GB006671.
- 33

- 1 22. Tank, S.E., Raymond, P.A., Striegl, R.G., McClelland, J.W., Holmes, R.M., Fiske, G.J. and Peterson,
2 B.J., 2012. A land-to-ocean perspective on the magnitude, source and implication of DIC flux from
3 major Arctic rivers to the Arctic Ocean. *Global Biogeochemical Cycles*, 26, GB4018.
- 4
- 5 23. Guo, L., Cai, Y., Belzile, C. and Macdonald, R.W., 2012. Sources and export fluxes of inorganic and
6 organic carbon and nutrient species from the seasonally ice-covered Yukon
7 River. *Biogeochemistry*, 107, 187-206.
- 8
- 9 24. Calmels, D., Gaillardet, J., Brenot, A., and France-Lanord, C., 2007, Sustained sulfide oxidation by
10 physical erosion processes in the Mackenzie River basin: Climatic perspectives: *Geology*, 35, 1003–
11 1006.
- 12
- 13 25. Horan, K., Hilton, R.G., Dellinger, M., Tipper, E., Galy, V., Calmels, D., Selby, D., Gaillardet, J.,
14 Ottley, C.J., Parsons, D.R. and Burton, K.W., 2019. Carbon dioxide emissions by rock organic
15 carbon oxidation and the net geochemical carbon budget of the Mackenzie River Basin. *American
16 Journal of Science*, 319, 473-499.
- 17
- 18 26. Raymond, P.A., Bauer, J.E., Caraco, N.F., Cole, J.J., Longworth, B. and Petsch, S.T., 2004. Controls
19 on the variability of organic matter and dissolved inorganic carbon ages in northeast US
20 rivers. *Marine chemistry*, 92, 353-366.
- 21
- 22 27. Soulet, G., Hilton, R.G., Garnett, M.H., Roylands, T., Klotz, S., Croissant, T., Dellinger, M. and Le
23 Bouteiller, C., 2021. Temperature control on CO₂ emissions from the weathering of sedimentary
24 rocks. *Nature Geoscience*, 14, 665-671.
- 25
- 26 28. Trumbore, S., 2000. Age of soil organic matter and soil respiration: radiocarbon constraints on
27 belowground C dynamics. *Ecological applications*, 10, 399-411.
- 28
- 29 29. Chen, C.T.A., Huang, T.H., Fu, Y.H., Bai, Y. and He, X., 2012. Strong sources of CO₂ in upper
30 estuaries become sinks of CO₂ in large river plumes. *Current Opinion in Environmental
31 Sustainability*, 4, 179-185.
- 32

- 1 30. Raymond, P.A., Hartmann, J., Lauerwald, R., Sobek, S., McDonald, C., Hoover, M., Butman, D.,
2 Striegl, R., Mayorga, E., Humborg, C. and Kortelainen, P., 2013. Global carbon dioxide emissions
3 from inland waters. *Nature*, 503, 355-359.
- 4
- 5 31. Ishikawa, N.F., Tayasu, I., Yamane, M., Yokoyama, Y., Sakai, S. and Ohkouchi, N., 2015. Sources
6 of dissolved inorganic carbon in two small streams with different bedrock geology: insights from
7 carbon isotopes. *Radiocarbon*, 57, 439-448.
- 8
- 9 32. Marwick T.R., Tamoooh F., Teodoru C.R., Borges A.V., Darchambeau F., Bouillon S., 2015. The age
10 of river-transported carbon: A global perspective. *Glob. Biogeochem. Cycle*. 29, 122-137.
- 11
- 12 33. Vihermaa, L.E., Waldron, S., Garnett, M.H. and Newton, J., 2014. Old carbon contributes to aquatic
13 emissions of carbon dioxide in the Amazon. *Biogeosciences*, 11, 3635-3645.
- 14
- 15 34. Ding, L., Qi, Y., Shan, S., Ge, T., Luo, C. and Wang, X., 2020. Radiocarbon in dissolved organic and
16 inorganic carbon of the South China Sea. *Journal of Geophysical Research: Oceans*, 125, JC016073.
- 17
- 18 35. Vaughn, L.J. and Torn, M.S., 2018. Radiocarbon measurements of ecosystem respiration and soil
19 pore-space CO₂ in Utqiagvik (Barrow), Alaska. *Earth System Science Data*, 10, 1943-1957.
- 20
- 21 36. Han, L.F. and Plummer, L.N., 2016. A review of single-sample-based models and other approaches
22 for radiocarbon dating of dissolved inorganic carbon in groundwater. *Earth-Science Reviews*, 152,
23 119-142.
- 24
- 25 37. Doctor, D.H., Kendall, C., Sebestyen, S.D., Shanley, J.B., Ohte, N. and Boyer, E.W., 2008. Carbon
26 isotope fractionation of dissolved inorganic carbon (DIC) due to outgassing of carbon dioxide from a
27 head water stream. *Hydrological Processes: An International Journal*, 22, 2410-2423
- 28
- 29 38. Marlier JF, O'Leary MH. 1984. Carbon kinetic isotope effects on the hydration of carbon
30 dioxide and the dehydration of bicarbonate ion. *Journal of the American Chemical Society*, 106,
31 5054 – 5057.
- 32

- 1 39. Griffith, D.R., McNichol, A.P., Xu, L., McLaughlin, F.A., Macdonald, R.W., Brown, K.A. and
2 Eglinton, T.I., 2012. Carbon dynamics in the western Arctic Ocean: insights from full-depth carbon
3 isotope profiles of DIC, DOC, and POC. *Biogeosciences*, 9, 1217-1224.
- 4
- 5 40. Wang, W., Zhong, J., Li, S.L., Ulloa-Cedamano, F., Xu, S., Chen, S., Lai, M. and Xu, S., 2023.
6 Constraining the sources and cycling of dissolved inorganic carbon in an alpine river, eastern
7 Qinghai-Tibet Plateau. *Science of The Total Environment*, 166262.
- 8
- 9 41. Roylands, T., Hilton, R.G., Garnett, M.H., Soulet, G., Newton, J.A., Peterkin, J.L. and Hancock, P.,
10 2022. Capturing the short-term variability of carbon dioxide emissions from sedimentary rock
11 weathering in a remote mountainous catchment, New Zealand. *Chemical Geology*, 608, 121024.
- 12
- 13 42. Vonk, J.E., Tank, S.E. and Walvoord, M.A., 2019. Integrating hydrology and biogeochemistry across
14 frozen landscapes. *Nature Communications*, 10, 5377.
- 15
- 16 43. Jessen, S., Holmslykke, H.D., Rasmussen, K., Richardt, N. and Holm, P.E., 2014. Hydrology and
17 pore water chemistry in a permafrost wetland, Ilulissat, Greenland. *Water resources research*, 50,
18 4760-4774.
- 19
- 20 44. Tank, S.E., Fellman, J.B., Hood, E. and Kritzberg, E.S., 2018. Beyond respiration: Controls on
21 lateral carbon fluxes across the terrestrial-aquatic interface. *Limnology and Oceanography Letters*, 3,
22 76-88.
- 23
- 24 45. Smith, S. L., Chartrand, J., Duchesne, C., Smith, S. L., Chartrand, J., & Duchesne, C. 2018. Report
25 on 2017 field activities and collection of ground-thermal and active-layer data in the Mackenzie
26 corridor, Northwest Territories; *Geological Survey of Canada*, 8492.
- 27
- 28 46. Lamontagne-Hallé, P., McKenzie, J. M., Kurylyk, B. L., & Zipper, S. C. 2018. Changing
29 groundwater discharge dynamics in permafrost regions. *Environmental Research Letters*, 13,
30 084017.
- 31
- 32 47. Liljedahl, A. K., Boike, J., Daanen, R. P., Fedorov, A. N., Frost, G. V., Grosse, G., et al. 2016.
33 Pan-Arctic ice-wedge degradation in warming permafrost and its influence on tundra hydrology.
34 *Nature Geoscience*, 9, 312–318.
- 35

- 1 48. Teufel, B., & Sushama, L. 2019. Abrupt changes across the Arctic permafrost region endanger
2 northern development. *Nature Climate Change*, 9, 858–862.
- 3
- 4 49. Walvoord, M. A., Voss, C. I., Ebel, B. A., & Minsley, B. J. 2019. Development of perennial thaw
5 zones in boreal hillslopes enhances potential mobilization of permafrost carbon. *Environmental*
6 *Research Letters*, 14, 015003.
- 7
- 8 50. Vaughn, L.J. and Torn, M.S., 2019. ^{14}C evidence that millennial and fast-cycling soil carbon are
9 equally sensitive to warming. *Nature Climate Change*, 9, 467-471.
- 10
- 11 51. Gareis, J.A. and Lesack, L.F., 2020. Ice-out and freshet fluxes of CO_2 and CH_4 across the air–water
12 interface of the channel network of a great Arctic delta, the Mackenzie. *Polar Research*, 39, 3528.
- 13
- 14 52. Hendy CH. 1971. The isotopic geochemistry of speleothems — I. The calculation of the effects
15 of different modes of formation on the isotopic composition of speleothems and their applicability
16 as palaeo climatic indicators. *Geochimica et Cosmochimica Acta*, 35, 801 – 824.
- 17
- 18 53. Michaelis J, Usdowski E, Menschel G. 1985. Partitioning of ^{13}C and ^{12}C on the degassing of
19 CO_2 and the precipitation of calcite — Rayleigh-type fractionation and a kinetic model.
20 *American Journal of Science*, 285, 318 – 327.
- 21
- 22 54. Campeau, A., Wallin, M.B., Giesler, R., Löfgren, S., Mörrh, C.M., Schiff, S., Venkiteswaran, J.J. and
23 Bishop, K., 2017. Multiple sources and sinks of dissolved inorganic carbon across Swedish streams,
24 refocusing the lens of stable C isotopes. *Scientific Reports*, 7, 9158.
- 25
- 26 55. Palmer SM, Hope D, Billett MF, Dawson JJ, Bryant CL. 2001. Sources of organic and inorganic
27 carbon in a headwater stream: Evidence from carbon isotope studies. *Biogeochemistry* 52, 321 – 338.
- 28
- 29 56. Mook WG, Bommerson JC, Staverman WH. 1974. Carbon isotope fractionation between
30 dissolved bicarbonate and gaseous carbon dioxide. *Earth and Planetary Science Letters*, 22, 169
31 – 176.
- 32
- 33 57. Zhang J, Quay PD, Wilbur DO. 1995. Carbon isotope fractionation during gas-water
34 exchange and dissolution of CO_2 . *Geochimica et Cosmochimica Acta*, 59, 107 – 114.

- 1
- 2 58. Szaran J. 1997. Achievement of carbon isotope equilibrium in the system $\text{HCO}_3(\text{solution})$ -
- 3 $\text{CO}_2(\text{gas})$. *Chemical Geology*, 142, 79 – 86.
- 4
- 5 59. Stuiver, M. and Polach, H.A., 1977. Discussion reporting of ^{14}C data. *Radiocarbon*, 19, 355-363.
- 6
- 7 60. Striegl, R.G., Dornblaser, M.M., McDonald, C.P., Rover, J.A. and Stets, E.G., 2012. Carbon dioxide
- 8 and methane emissions from the Yukon River system. *Global Biogeochemical Cycles*, 26, GB0E05.
- 9
- 10 61. Knapp, W.J. and Tipper, E.T., 2022. The efficacy of enhancing carbonate weathering for carbon
- 11 dioxide sequestration. *Frontiers in Climate*, 4, 928215.
- 12
- 13 62. Li, S., Li, G.K., Li, W., Chen, Y., Raymo, M.E. and Chen, J., 2023. Effects of secondary carbonate
- 14 precipitation and dissolution on Changjiang (Yangtze) river chemistry and estimates of silicate
- 15 weathering rates. *Global Biogeochemical Cycles*, 2022GB007581.
- 16
- 17 63. Bryant, C.L., Henley, S.F., Murray, C., Ganeshram, R.S. and Shanks, R., 2013. Storage and
- 18 hydrolysis of seawater samples for inorganic carbon isotope analysis. *Radiocarbon*, 55, 401-409.
- 19
- 20 64. General-Statement-of-14C-Procedures_2023.pdf (whoi.edu) [www2.whoi.edu/site/nosams/wp-](http://www2.whoi.edu/site/nosams/wp-content/uploads/sites/124/2023/02/General-Statement-of-14C-Procedures_2023.pdf)
- 21 [content/uploads/sites/124/2023/02/General-Statement-of-14C-Procedures_2023.pdf](http://www2.whoi.edu/site/nosams/wp-content/uploads/sites/124/2023/02/General-Statement-of-14C-Procedures_2023.pdf).
- 22
- 23 65. Andersson, A. 2011. A systematic examination of a random sampling strategy for source
- 24 apportionment calculations. *Sci. Tot. Environ.*, 412, 232–238.
- 25
- 26 66. Parnell, A.C.; Inger, R.; Bearhop, S.; Jackson, A. L, 2010. Source apportionment using stable
- 27 isotopes: coping with too much variation. *PLOS one*, 5, 1-5.
- 28
- 29 67. Andersson, A.; Deng, J; Ke. D.; Zheng, M.; Yan, C.; Sköld, M.; Gustafsson, Ö, 2015. Regionally-
- 30 varying combustion sources of the January 2013 severe haze events over eastern China. *Environ. Sci.*
- 31 *Technol.* 49, 2038–4496.
- 32
- 33 68. Dasari, S., Andersson, A., Popa, M.E., Rockmann, T., Holmstrand, H., Budhavant, K. and
- 34 Gustafsson, O., 2021. Observational evidence of large contribution from primary sources for carbon
- 35 monoxide in the South Asian outflow. *Environmental Science & Technology*, 56, 165-174.

- 1
- 2 69. Dasari, S., Andersson, A., Stohl, A., Evangeliou, N., Bikkina, S., Holmstrand, H., Budhavant, K.,
- 3 Salam, A. and Gustafsson, O., 2020. Source quantification of South Asian black carbon aerosols with
- 4 isotopes and modeling. *Environmental Science & Technology*, 54, 11771-11779.
- 5
- 6 70. Dasari, S., Paris, G., Saar, B., Pei, Q., Cong, Z. and Widory, D., 2022. Sulfur isotope anomalies
- 7 ($\Delta^{33}\text{S}$) in urban air pollution linked to mineral-dust-associated sulfate. *Environmental Science &*
- 8 *Technology Letters*, 9, 604-610.
- 9
- 10 71. Bosch, C.; et al 2015. Source Apportionment of Polycyclic Aromatic Hydrocarbons in Central
- 11 European Soils with Compound-Specific Triple Isotopes (^{13}C , ^{14}C , and ^2H). *Environ. Sci. and*
- 12 *Technol.* 49, 7657-7665.
- 13
- 14 72. Tesi, T.; et al., 2016 Massive remobilization of permafrost carbon during post-glacial warming. *Nat.*
- 15 *Commun.* 7, 13653.
- 16
- 17 73. Wheeler, J. O., Hoffman, P. F., Card, K. D., Davidson, A., Sanford, B. V., Okulitch, A. V., and
- 18 Roest, W. R., 1996, Geological map of Canada: Natural Resources Canada.
- 19
- 20 74. Schwab, M.S., Hilton, R.G., Haghypour, N., Baronas, J.J. and Eglinton, T.I., 2022. Vegetal
- 21 undercurrents—Obscured riverine dynamics of plant debris. *Journal of Geophysical Research:*
- 22 *Biogeosciences*, 127, 2021JG006726.
- 23
- 24 75. Graven, H., Keeling, R.F. and Rogelj, J., 2020. Changes to carbon isotopes in atmospheric CO_2 over
- 25 the industrial era and into the future. *Global Biogeochemical Cycles*, 34, GB006170.
- 26

Figure Captions

27 **Figure 1. The Mackenzie River Basin and sampling locations of this study.** (A) Elevation (GDEM

28 30 Arc Second) shown with river sampling locations. (B) Bedrock geology of the sampling area,

29 coded by major rock type⁷³. Continuous permafrost dominates these locations⁷⁴.

30

31 **Figure 2. The controls on DIC isotope composition in the Mackenzie River Basin.** Pathways of

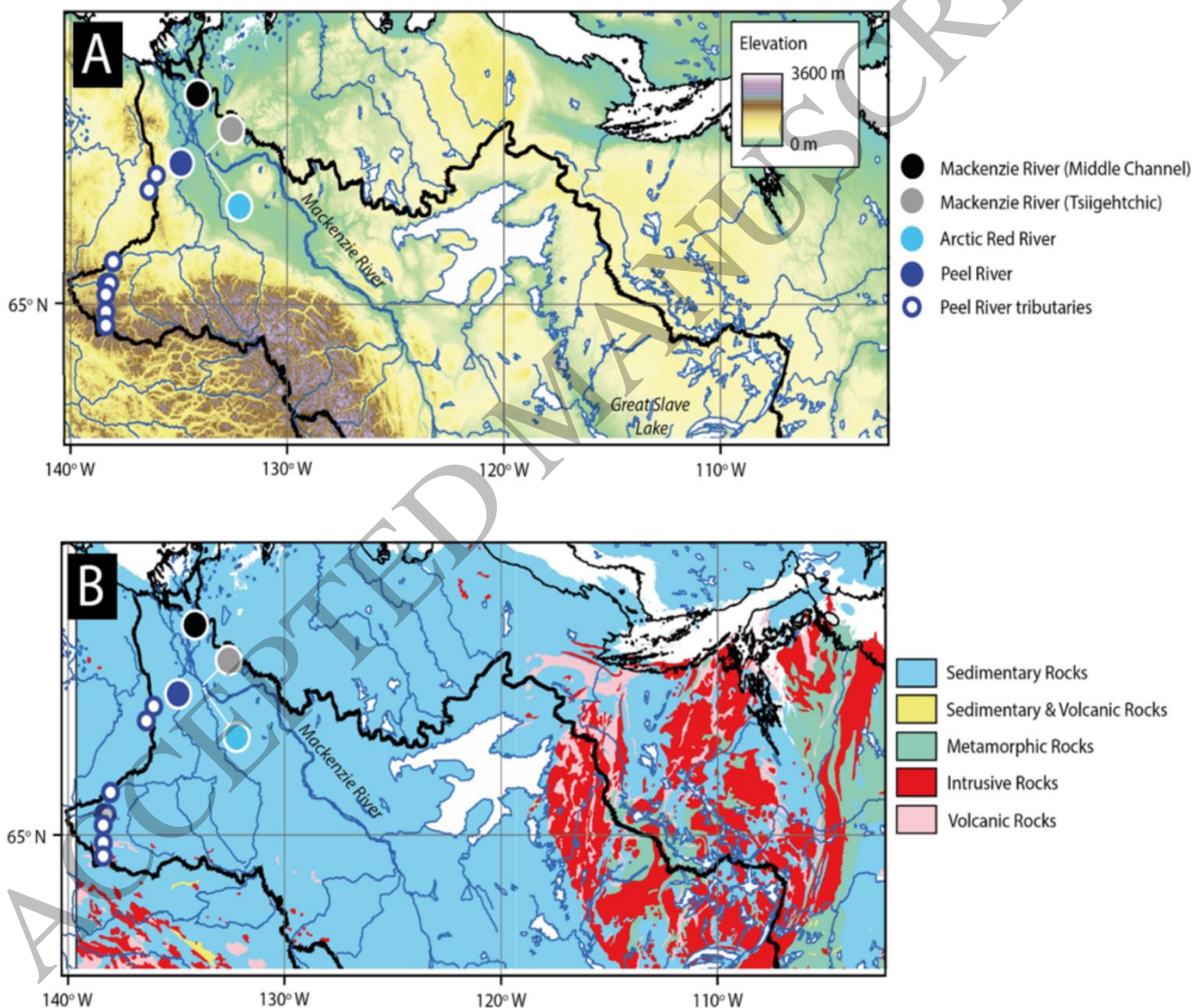
32 atmospheric CO_2 (blue), C from the vegetation and soil (green), C from rock organic matter and

1 carbonate minerals (grey) and mixtures of these sources (pink) are conceptualised. Permafrost present
2 in bedrock and peat and soil is shown shaded white. DIC can be produced by rock weathering (1),
3 introducing atmospheric and geological C into the river DIC pool. Ecosystem respiration produces
4 CO₂ (2), and this can contribute to the DIC pool in the landscape, and sources 1 + 2 can be moved by
5 hydrological pathways to the river network. Atmospheric exchange may act to modify the DIC
6 isotope composition (3), while CO₂ evasion from river surfaces (4) will impact the stable isotope
7 composition.

8
9 **Figure 3. Dual isotope characteristics of DIC in the Mackenzie River system. A.** New river DIC
10 measurements (diamonds; ‘black filled’ – Mackenzie River Middle Channel, ‘grey filled’ –
11 Mackenzie River at Tsiigehtchic, ‘cyan filled’ – Arctic Red River, ‘blue filled’- Peel River, ‘open’ –
12 Peel River Tributaries) are shown alongside measurements that characterise potential sources of
13 carbon to the DIC pool which include river particulate organic carbon (POC, triangle)¹⁸, dissolved
14 organic carbon (DOC, squares)¹⁷, soil CO₂ (circles)³⁵ and atmospheric CO₂ (pentagons) from Point
15 Barrow⁷⁵. **B.** The range of carbon compositions that capture biospheric organic matter oxidation are
16 shaded green, alongside an inferred end member and standard deviation on compositions (circle,
17 Table S3). The endmember compositions of weathering are shown. DIC_{predicted} is the result of the
18 previously quantified chemical weathering fluxes^{24,25} coupled to their isotopic endmembers (mixing
19 components shown as grey dotted line, Table S4). The expected trajectory for a two-component
20 mixing (chemical weathering and biosphere organic carbon oxidation) is shown (black line).

21 **Figure 4. The influence of chemical weathering on the Mackenzie River DIC radiocarbon**
22 **content.** The ratio of the weathering products from carbonate and sulfide mineral weathering i.e.,
23 water-soluble ion concentrations, are shown normalized to DIC concentrations, along with the
24 radiocarbon content of the DIC for: A) calcium and sulphate ions; and B) calcium and magnesium
25 ions. Blue shaded region denotes zone of compositions produced by theoretical carbonate weathering
26 reactions by carbonic (H₂CO₃) and sulfuric acid (H₂SO₄). Samples lie outside this domain and suggest
27 the potential role of both isotopic exchange with atmospheric CO₂ and addition of DIC with a higher
28 $\Delta^{14}\text{C}$ value than weathering inputs. Linear fits and 95% confidence interval are shown as dashed lines,
29 and suggest addition of DIC while $\Delta^{14}\text{C}$ increases.

1 **Figure 5. Role of CO₂ evasion from the Mackenzie River system on DIC stable isotope**
 2 **composition.** (A) The mixing triangle is shown comprising of three likely sources of DIC in this river
 3 system (symbols as per Figure 3). DIC_{prior} is estimated based on the expected maximum isotopic
 4 fractionation due to CO₂ release. The ‘Biosphere organic carbon oxidation’ isotopic endmember is a
 5 mix of river POC and CO₂ soil pore isotopic signatures shown in Figure 3 with equal weightages given
 6 for both (see Discussion) (B) The relation between excess *PCO*₂ is shown with the δ¹³C signature of
 7 DIC in this river system. The estimated uncertainty in calculation of the *PCO*₂ is 10% similar to
 8 previous study³⁷. (C) The relative source contributions to DIC_{prior} is shown.



9 **Figure 1**

10 *Figure 1*
 11 178x172 mm (DPI)

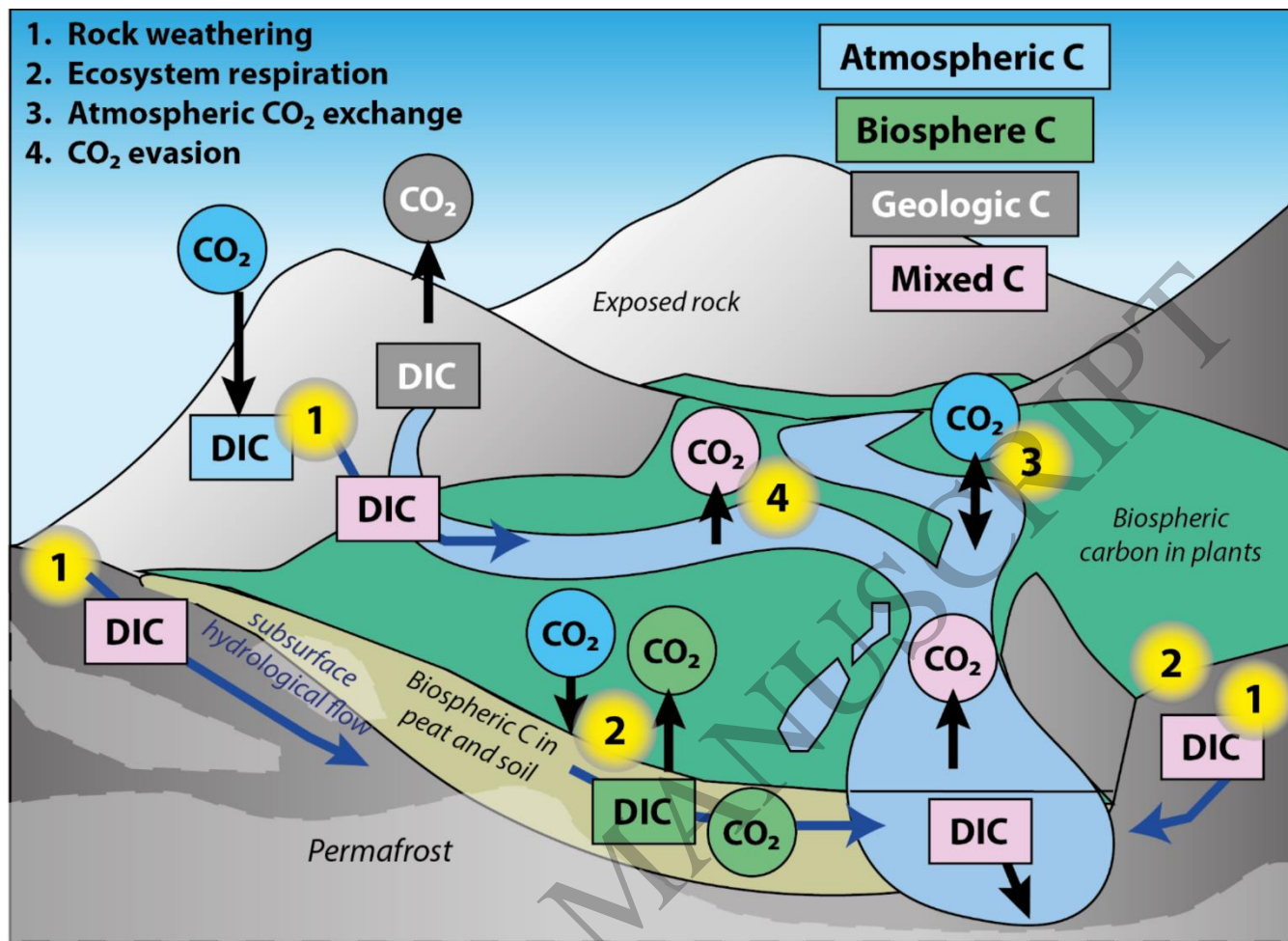


Figure 2

Figure 2
177x143 mm (DPI)

1
2
3
4

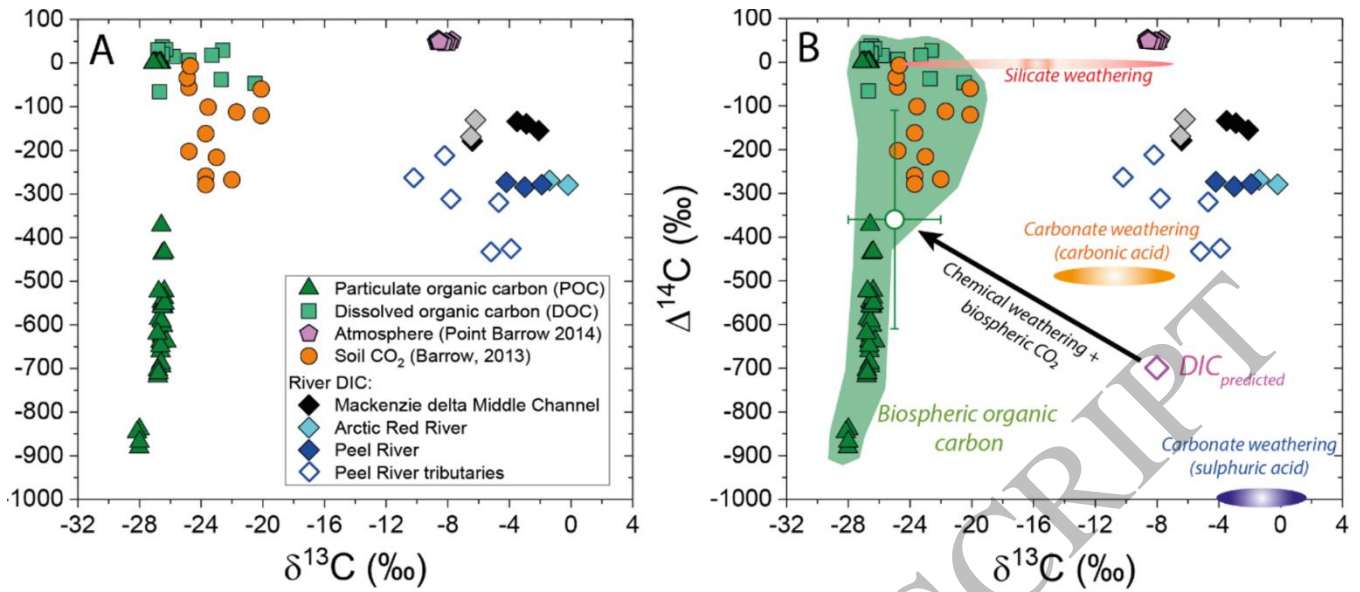


Figure 3

Figure 3
177x93 mm (DPI)

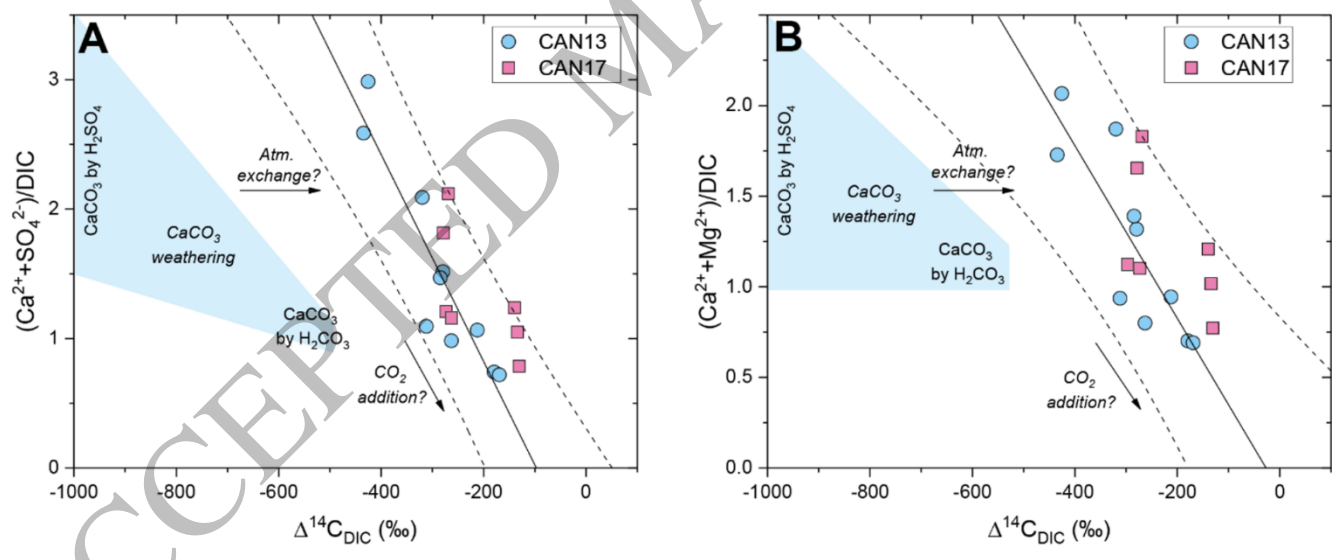


Figure 4

Figure 4
177x88 mm (DPI)

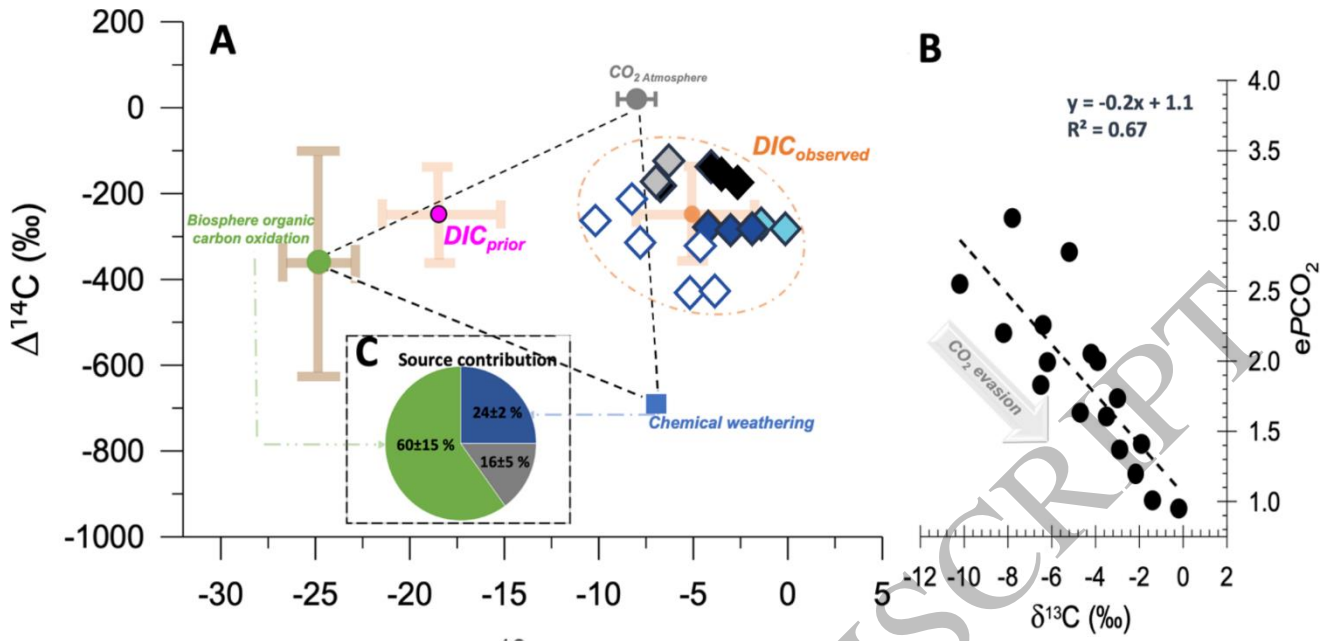


Figure 5

Figure 5
173x99 mm (DPI)

1
2
3